Science of the Total Environment 831 (2022) 154879

Contents lists available at ScienceDirect

Science of the Total Environment

journal homepage: www.elsevier.com/locate/scitotenv

Hydrodynamic and biogeochemical evolution of a restored intertidal oyster (*Crassostrea virginica*) reef

David Cannon [a,*], Kelly Kibler [a], Linda Walters [b], Lisa Chambers [b]

[a] Department of Civil, Environmental, and Construction Engineering and National Center for Integrated Coastal Research, University of Central Florida, Orlando, FL 32816, USA
[b] Department of Biology and National Center for Integrated Coastal Research, University of Central Florida, Orlando, FL 32816, USA

HIGHLIGHTS

- Hydrodynamic and biogeochemical changes were monitored after reef restoration.
- Lowering the reef crest immediately increased channel-to-reef hydraulic connectivity.
- Increases in oyster density enhanced sediment nutrients.
- Within-canopy turbulent energy and dissipation increased by >200% within 12 months.
- The restored reef was functionally similar to a reference reef within 1 year.

GRAPHICAL ABSTRACT

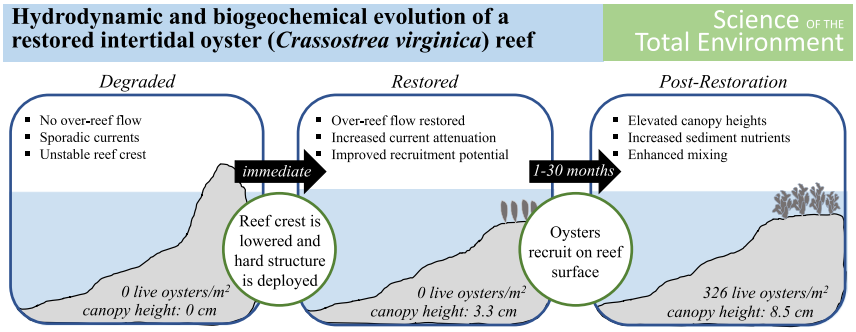

ARTICLE INFO

Editor: Ashantha Goonetilleke

Keywords:
Restoration
Estuary
Turbulence
Carbon
Nitrogen
Ecohydraulics

ABSTRACT

Oyster reef restoration is increasingly used as a tool for restoring lost ecosystem services in degraded aquatic systems, but questions remain about the efficacy of the practice and when/if restored reefs may behave similarly to intact natural reefs. In this case study, field observations highlighted short- (<1 month post-restoration) and longer-term (30 months; 3 recruitment cycles) transformations in canopy, hydrodynamic, and biogeochemical characteristics of a restored intertidal oyster reef relative to nearby intact and degraded reefs. Within 12 months of restoration, live oyster density (326 oysters/m^2), mean shell length (47 mm), and mean canopy height (76 mm) did not differ significantly from those observed on a reference reef. Lowering of the reef crest during restoration reestablished over-reef flow and periodic tidal inundation, improving hydraulic connectivity between the channel and the reef surface. This immediately restored much of the reef's hydrodynamic function and eliminated the irregular flow patterns observed on the previously degraded reef. Results showed that mean flow (channel-to-reef flow attenuation: 98% / 62%; within/above canopy) and velocity normalized turbulence ($\overline{w'^2}/U^2$: $10^{-1}/10^{-2}$; ϵ/U^3: $10^{0}/10^{-2}$ m^{-1}) characteristics were similar across the restored and reference reefs within 1 year of restoration, with temporal changes in mixing within the canopy attributed to increases in live oyster density. Nutrient pools (mean total carbon, total nitrogen) on reference and restored reefs had similar magnitudes within 1 year (C: 39 & 33 g/kg, N: 1.5 & 1.8 g/kg), while increases in DOC and NH_4^+ were correlated with the presence of live oysters. Most changes that occurred on the restored reef were linked to oyster recruitment and canopy growth, which modulated hydrodynamics through direct flow interactions and controlled sediment nutrient and organic matter content through waste deposition and burial.

1. Introduction

Shellfish populations have decreased substantially over the last century (>85%) as exogenous pressures (e.g. overharvesting, boating, pollution, increased predation) have precipitated oyster reef degradation around the

* Corresponding author.
E-mail address: David.Cannon@ucf.edu (D. Cannon).

http://dx.doi.org/10.1016/j.scitotenv.2022.154879
Received 8 November 2021; Received in revised form 23 March 2022; Accepted 24 March 2022
Available online 29 March 2022

globe (Beck et al., 2011). The loss of oyster habitat and its associated economic and ecological benefits have motivated restoration-focused policy initiatives worldwide (e.g. U.S. Estuary Restoration Act, United Nations Decade on Ecosystem Restoration) and there has been significant investment in restoration science in recent years (Blomberg et al., 2018). Efforts were historically aimed at improving the commercial fishing industry, which relies on oyster reefs for both direct harvesting (i.e. oyster provision) and foraging habitat (Coen and Luckenbach, 2000). Restoration goals have since shifted to broader ecosystem services, including water quality improvement (Dame et al., 1989), shoreline stabilization (Meyer et al., 1997; McClenachan et al., 2020), carbon and nutrient sequestration (Fodrie et al., 2017; Chambers et al., 2018), and enhancement of biodiversity (Loch et al., 2021). The breadth of ecosystem services associated with healthy reef habitats make them an attractive target for restoration initiatives, and coastal communities are increasingly turning to oyster reefs for ecosystem improvement (Hernández et al., 2018).

Significant progress has been made in developing successful oyster reef restoration and construction strategies over the last several decades. In the United States, reef restoration efforts have targeted shallow estuaries on the western Atlantic (*Chesapeake Bay*: Schulte et al., 2009; *Hudson-Raritan Estuary*: Holley et al., 2018; *Indian River Lagoon*: Garvis et al., 2015; *Back Sound*: Ridge et al., 2015; *Pamlico Sound*: Theuerkauf et al., 2019; Powers et al., 2009) and Gulf (*Caloosahatchee Estuary*: Barnes et al., 2007; *Mobile Bay*: Gregalis et al., 2008; *Apalachicola Bay*: Pine et al., 2015) coasts, where subtidal and intertidal reefs of *Crassostrea virginica* have historically dominated the aquatic landscape. Restoring these degraded oyster habitats generally involves installing artificial structures (manufactured or natural) on reef-mimicking bed forms to promote oyster recruitment, which requires hard substrate for successful spat attachment (Kennedy et al., 1996). Recruited oysters can then form complex three-dimensional surface layers, or canopies, on deployed structures, thus improving benthic habitats, enhancing biodiversity, and modulating hydrodynamics. This phase of restoration has received significant research scrutiny, with studies focused on the importance of structure choice (e.g. Goelz et al., 2020; Nitsch et al., 2021), habitat suitability (e.g. Theuerkauf and Lipcius, 2016; Wall et al., 2005), and substrate stability (e.g. Walters et al., 2021b).

Despite the initial success of many restoration efforts in recruiting oysters, little is known about the long-term stability or ecosystem impacts of reef restoration. Recent studies on the temporal evolution of ecosystem services on restored reefs, including the authors' own work, were largely designed using the space-for-time (SFT) experimental design. Using this approach, data are collected on multiple restored reefs of varying restoration ages and combined to investigate general differences related to time since restoration, which can then be used to infer the time required for restored reefs to produce desired ecosystem benefits (e.g. Chambers et al., 2018; Walters et al., 2021b). However, these studies are unable to describe short-term changes at restored reefs (i.e. within weeks or months of restoration), and the direct effects of restoration on any individual reef are often ignored in averaging. Reports on monitoring for individual restored reefs, where observations are collected both pre- and post-restoration, are sparse (exceptions: La Peyre et al., 2014), limiting the understanding of how ecosystem services evolve over short timescales, especially immediately following restoration. Additionally, most studies focus on only one aspect of the ecosystem services provided by restored reefs (e.g. biogeochemistry, biodiversity, etc.) rather than integrating multiple lines of research. Post-restoration hydrodynamic, biological, and chemical changes likely occur over months, or even years (e.g. La Peyre et al., 2013), and understanding the temporal evolution of these characteristics on the site scale is imperative for designing effective restoration and monitoring strategies, as well as evaluating the success of restoration projects (Elliott et al., 2007).

In this study, restoration-related changes in the physio-chemical and biological landscape of an intertidal oyster reef (*Crassostrea virginica*) are investigated in a shallow estuary along the Atlantic coast of Florida (USA). It is hypothesized that changes in hydrodynamics (e.g. flow attenuation, turbulence) and sediment biogeochemistry (e.g. organic matter, nutrients) on the restored reef are linked directly to oyster recruitment and canopy growth. Conditions were monitored for nearly three years, including pre- and post-restoration surveys, with additional monitoring conducted on nearby intact (reference condition) and degraded oyster reefs for reference. Hydrodynamic measurements were collected semi-annually within and above the oyster canopy, while reef characteristics (i.e. reef canopy height, live oyster density, etc.), sediment nutrients, and biodeposits were surveyed periodically over the observation period. This work is designed to highlight the evolution of a restored reef over time, providing the first case study integrating observations of oyster community, reef structure, hydrodynamics, and biogeochemical development over time since reef restoration.

2. Methods

2.1. Study area description

Experiments were conducted in Mosquito Lagoon, a shallow, microtidal estuary on the Atlantic coast of Florida, USA that is part of the Indian River Lagoon system (Fig. 1). Mosquito Lagoon has a mean water depth of 1.7 m and circulation is largely driven by winds and tides, which remain microtidal throughout much of the waterbody (range: 1 cm–1 m; 10 cm in study region). Exchange with the Atlantic Ocean and Indian River occurs through narrow inlets to the north and south, respectively. The lagoon is subject to long water residence times (mean water half-life: 76 days), high salinities, and, more recently, high nutrient loadings (Smith, 1993; Steward et al., 2006; Phlips et al., 2014). Lagoon water temperatures range from 4 to 33 °C, salinities range from 22.6 to 45.2 ppt, and vertical stratification is limited due to the shallowness of the estuary (Walters et al., 2001; Phlips et al., 2014). Relative sea level rise in Mosquito Lagoon averages 2 cm/yr (IRL NEP, 2020), in line with other observations along the southern Atlantic coast (2–4 cm/yr; https://tidesandcurrents.noaa.gov/sltrends/).

Intertidal shellfish reefs (predominantly Eastern oyster, *Crassostrea virginica*) are found primarily in the northernmost portion of the lagoon, where proximity to the ocean inlet enhances the tidal range (20–100 cm). The total aerial coverage of intertidal reefs in Mosquito Lagoon has declined substantially (>20%) over the last 50 years (Garvis et al., 2015), with studies suggesting that reef degradation is linked to recreational boat wakes, which are known to dislodge and destroy live oyster clusters (e.g. Grizzle et al., 2002; Walters et al., 2021b). Significant efforts have been made to restore intertidal oyster reefs and their associated ecosystem services throughout the lagoon, including more than 91 successful reef restorations (totaling >3.5 acres) performed by the authors (L.J. Walters, unpublished data).

Measurements were collected on three intertidal reefs of Eastern oyster (*C. virginica*) located in northern Mosquito Lagoon (Fig. 1). Sample reefs included [1] a reference-condition intact oyster reef (reference: area: 530 m^2), [2] an oyster reef that was restored at the onset of the study (restored; area: 94 m^2), and [3] a degraded reef with few live oysters (degraded; area: 240 m^2). The restored reef was selected at random from five reefs restored by the authors in 2018. The study design required extensive sampling on each reef, and including replicate reference, degraded, and restored reefs was infeasible. Elevation profiles on each reef were characteristic of their degradation status (Fig. 2a). While the reference reef had a wide plateau and maximum elevations below the mean high water depth, the degraded and restored (pre-restoration) reefs were characterized by steep, narrow crests that remained emergent over much, if not all, of the tidal cycle. Degradation at the restored and degraded reefs was linked to recreational boat wakes (e.g. Grizzle et al., 2002; Walters et al., 2021b), which dislodge live oysters from the bed and lead to shell piling and distinctive crest formation on the reef surface. These crests were present on the degraded reef throughout the study and on the restored reef prior to restoration, at which time the reef was manually regraded (discussed below). Importantly, the reference and degraded reefs were unconfounded by previous restoration attempts, allowing them to act as control sites for all hydrodynamic and biogeochemical measurements.

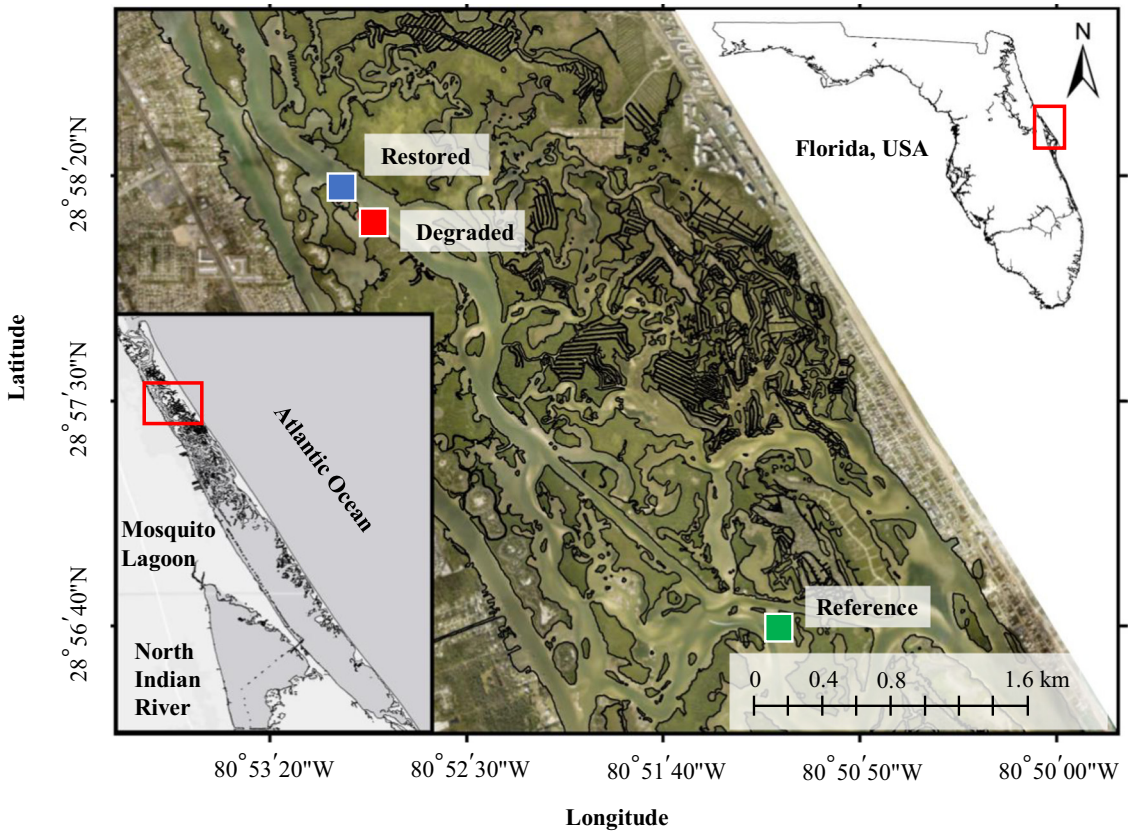

Fig. 1. Map of study area with study reefs displayed as colored squares (Restored: blue; Degraded: red; Reference: green). Inset diagrams show the study area location in relation to Mosquito Lagoon and Florida, USA.

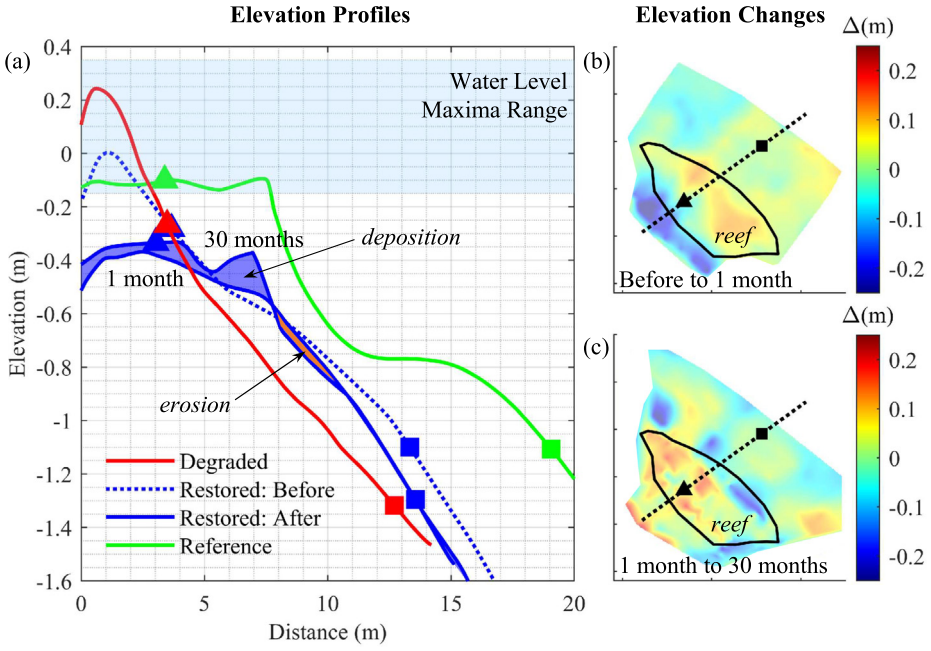

Fig. 2. Cross-sectional elevation profiles (a: all reefs) and elevation changes (b–c: restored reef) for Degraded (red), Reference (green), and Restored (blue) sample reefs. Elevation profiles on the Restored reef were measured both before (dotted) and after (solid) restoration took place. Post-restoration elevation changes on the restored reef (1 month–30 months) are indicated with shading in subplot (a), while changes over the entire reef footprint are displayed using colored shading in (b: before–1 month) and (c: 1 month–30 months). Markers represent the locations of velocity profiles measured on-reef (triangles) and in the channel (squares), and the horizontal band in (a) shows the range of observed water level maxima.

Reef restoration at the restored site took place in June 2018 following an initial characterization of pre-restoration conditions at the reef. Shells and sediments on the reef crest were manually graded offshore using landscape rakes (Fig. 2a,b). This process stabilized the reef surface and lowered maximum elevations to low intertidal height, facilitating periodic inundation and oyster recruitment. Oyster mats made of Vexar™ extruded polyethylene mesh (50 cm × 50 cm) were deployed across the reef surface and anchored with small (diameter: ~15 cm) concrete irrigation weights (~2.5 kg) to improve stability. Oyster mats were constructed using 36 vertically oriented adult *C. virginica* shells attached using zip-ties, with shells positioned in such a way that they mimicked the structure of live reefs. Oyster mats were specifically designed to promote natural oyster recruitment and increase resiliency to boat-wakes using mechanically stabilized shells (Garvis et al., 2015). Oyster recruitment occurred naturally, and no artificial larvae seeding was used to propagate the reef. Much of the restoration work was conducted by volunteers, with over 61,000 volunteers participating in restoration initiatives in Mosquito Lagoon over the last decade (Hawthorne et al., 2022). This restoration was completed with a total budget under $6000 and required approximately 100 volunteer hours for preparation and deployment (Linda Walters, pers. com.). Although beyond the scope of this study, information on community response and sense of place regarding restoration projects in the region can be found in Hawthorne et al. (2022).

2.2. Field observations

2.2.1. Oyster reef characterization

Study reefs were monitored for live oyster density, shell length, and canopy height less than one week before restoration occurred, and at 1, 6, 12, and 30 months post-restoration. All parameters were sampled using haphazardly placed 50 cm × 50 cm quadrats (0.25 m^2). Quadrat locations on the reefs were haphazardly selected by the research team at low tide by having individuals close their eyes and throw quadrats. Oyster shell length was measured in mm with calipers (or rulers) for 50 *C. virginica* in each of five quadrats, with averages computed over each quadrat for use in statistical analyses. The same quadrats were also used to determine the density by counting all live *C. virginica* in each quadrat. On each of ten haphazardly selected quadrats per reef, the height of the oyster canopy was recorded at five haphazardly selected points using a metal rod (rod diameter: 1 mm) inserted into the substrate to the point of first resistance. The distance between the tip of the rod and the top of the tallest nearby oyster or shell was measured with a ruler and all measurements in a single quadrat were averaged for analysis. The canopy height is used to track fine-scale, vertical accretion above the sediment over time (e.g. Walters et al., 2021a), with the expectation that reefs will continue to increase in height via oyster growth and recruitment until they reach the maximum for growth enabled by the local tidal range (Rodriguez et al., 2014).

Reef elevations and offshore bathymetry were measured using a CHC X91+ real time kinematic (RTK) GNSS surveyor prior to restoration on all three reefs. Post-restoration surveys were completed on the restored reef immediately after restoration and after approximately 30 months. Point measurements were collected on the reef surface (i.e. within the oyster canopy) and in the adjacent channel using a topo shoe, and GPS elevations were converted to NAVD-88 using an elevation benchmark located within 2 km of the sample reefs.

2.2.2. Hydrodynamics

Hydrodynamic characteristics were monitored before and after restoration on all reefs to assess the impact of reef alterations on mean flow and turbulence. Preliminary observations were collected on the restored reef approximately 1 week before restoration, followed by four additional post-restoration observations conducted at the restored, reference, and degraded reefs (time since restoration: 1 month, 6 months, 12 months, 30 months). On each observation date, current velocities were measured concurrently near the reef crest and offshore in the adjacent channel (10–15 m from reef crest). Hydrodynamic measurements on the degraded reef were collected on the channel-ward slope of the reef crest (Fig. 2a), as the crest of the degraded reef was rarely submerged. Measurement locations were selected such that the surrounding roughness elements (i.e. oyster canopy or disarticulated shell) were representative of the larger reef surface and water depths were large enough to submerge the velocity probe. Measurements were collected continuously for 2–4 h during the flood tide when the flow speeds were approximately steady. On-reef velocity profiles were sampled at 100 Hz using a Nortek Vectrino Profiler, with measurements collected within (before, 1 month, 12 months) and above (6 months, 30 months) the oyster canopy during alternating observation periods. Velocity profiles (3 cm range; 1 mm resolution) were positioned such that the most accurate portion of the profile (5 cm below the probe; Thomas et al., 2017) was located approximately 2 cm and 9.5 cm above the bottom for within and above canopy measurements, respectively. Following each deployment, local oyster canopy characteristics, including reef-element densities and cluster heights, were measured within a 0.25 m^2 quadrat centered approximately 25 cm directly upstream of the velocity probe. Offshore channel velocities were measured using a 2 MHz Nortek Aquadopp HR Profiler (sample rate 2 Hz) deployed in a down-looking orientation near the water surface. Velocity profiles were resolved within at least 50 cm of the bed (2 cm resolution), and the channel bottom was identified using instrument-measured signal amplitude profiles (e.g. Kitsikoudis et al., 2020). Both velocimeters were aligned to a common coordinate system in the field, such that $\overline{u}$, $\overline{v}$, and $\overline{w}$ represented mean reef-parallel, cross-shore, and vertical velocity components, respectively.

Meteorological conditions were monitored during each deployment to characterize hydrodynamic forcing. Wind speeds and directions were measured using a Davis Wind Speed and Direction Smart Sensor (Onset; 60 s interval) mounted approximately 2 m above the water surface in the main channel, and offshore water depths were measured using a pressure logger (Onset U20L-04) deployed near the Aquadopp HR Profiler. Water surface deformations were measured continuously (sample rate: 32 Hz) on the reef and in the main channel using sonic water surface loggers (Ocean Sensor Systems XB Pro), with time series used to calculate significant wave heights ($H_s = 4\sigma_s$) over 2-minute (50% overlap) data segments (Dean and Dalrymple, 1991).

2.2.3. Biogeochemistry

Sediment biogeochemical properties on the three reefs were quantified at approximately 1, 6, 12, and 24 months following restoration. Sampling of sediment for biogeochemical analysis took place during low tide (when the reef was exposed) to prevent sediment resuspension. Four unique sampling points were chosen on each reef during each sampling event by haphazardly placing a soil core tube while walking along the reef surface; at each sampling point, duplicate 0–5 cm deep sediment cores were collected using a 7 cm diameter polycarbonate tube beveled on the end and hammered into the sediment, using care to avoid large shells. Sediments were field-extruded and stored in air-tight polyethylene bags on ice during transport to the laboratory, where all samples were weighed, large pieces of shell (>2 cm diameter) were removed, and the duplicate cores from each sampling point were combined and homogenized by hand, resulting in four samples per reef. At all sampling times, ~100 g wet weight sediment was oven dried at 70 °C until constant weight and ground in a stainless-steel ball mill (SPEX Sample Prep 8000M Mixer/Mill. SPEX, Metuchen, NJ) to particle size. A subsample was combusted at 550 °C for 5 h to determine organic matter (OM) content via loss-on-ignition (LOI). Following combustion, the remaining ash was boiled in 1 M HCl for 1 h, filtered through Whatman #41 filter paper, and analyzed for total phosphorus (P) on a Seal AQ2 (Seal Analytical, Mequon, WI) following method 365.1 Rev. 2.0 (Andersen, 1976; USEPA, 1993). A second sediment subsample was used to determine total carbon (C) and nitrogen (N) on a Vario Micro Cube CN Analyzer (Elementar Americas Inc., Mount Laurel, NJ). At the 24-month sampling, additional analyses included extractable nutrients: nitrate (NO_3^-), ammonium (NH_4^+), soluble reactive phosphorus (SRP), and dissolved organic C (DOC). Extractable nutrients were processed within 72 h of sample collection and involved placing ~4 g field moist sediment in a

40 mL centrifuge tube with 25 mL 2 M KCl. Samples were mixed on an orbital shaker at 100 rpm for 1 h, then centrifuged at 4000 rpm at 10 °C for 10 min. The supernatant was filtered through a 0.45 μm membrane filter, acidified to pH < 2 with H_2SO_4, and stored at 4 °C until analysis. Concentrations of NO_3^-, NH_4^+ and SRP were determined colorimetrically on a Seal AQ2 Automated Discrete Analyzer (Seal Analytical, Mequon, WI) using EPA methods 353.2 Rev. 2.0, 350.1 Rev. 2.0, and 365.1 Rev. 2.0, respectively (USEPA, 1993). A Shimadzu TOC-L Analyzer (Shimadzu Scientific Instruments, Kyoto, Japan) was used to measure the concentration of nonpurgeable DOC.

2.3. Data analysis

2.3.1. Hydrodynamic analysis

All velocity measurements were quality controlled to remove data with low correlations (<80%) and poor signal-to-noise ratios (SNR < 20). Data gaps were subsequently replaced via linear interpolation, and time series were despiked using a phase-space thresholding algorithm (Goring and Nikora, 2002; Wahl, 2003). Velocity measurements collected near the bed in the main channel (<5 cm above bottom) were removed due to acoustic backscatter contamination, and values were replaced using linear interpolation and an assumption of a no-slip condition at the bed. Additionally, all data affected by boat wakes were noted in the field and excluded from analysis. Mean velocity profiles were estimated from quality-controlled time series in 120 s (50% overlap) data segments, over which the flow was assumed stationary. Depth integrated reef-parallel and cross-shore channel velocities ($\overline{u_{CH}}$, $\overline{v_{CH}}$) were computed using offshore velocity profiles, with integration limited to the bottommost 50 cm of the water column for consistency across experiments. Channel-to-reef velocity attenuation (η_U) was estimated as the slope of the best-fit (i.e. least squares) line $\overline{U_R} = \eta_U * \overline{U_{CH}} + b$, where $\overline{U_{CH}} = \left(\overline{u_{CH}}^2 + \overline{v_{CH}}^2\right)^{1/2}$ and $\overline{U_R} = \left(\overline{u_R}^2 + \overline{v_R}^2\right)^{1/2}$ are the total horizontal current speeds measured in the channel and above the reef in the velocity profile midpoint and b is the intercept.

Velocity time series collected on the reef were used to calculate wave-removed estimates of the Reynolds stress tensor. Energy contributions from waves and turbulence were separated using the phase method, which allows for wave-turbulence decomposition in spectral space (e.g. Bricker and Monismith, 2007). Power spectral density functions were estimated for individual velocity components (u, v, w), and the energy contributions from waves and turbulence were separated using a best-fit line interpolated across the surface-wave frequency band (0.3 Hz < f < 2 Hz). Wave-removed estimates of the auto- ($\overline{u'^2}$, $\overline{v'^2}$, $\overline{w'^2}$) and cross-correlation ($\overline{u'w'}$, $\overline{v'w'}$, $\overline{u'v'}$) terms of the Reynolds stress tensor were further refined by removing energy associated with acoustic Doppler noise, as described in Thomas et al. (2017). Strong wave-induced velocity fluctuations in the horizontal velocity plane (u, v) produced large biases in the associated turbulent energy estimates (e.g. Hansen and Reidenbach, 2017). Consequently, analysis was limited to vertical turbulent energy ($\overline{w'^2}$) and cross-correlation ($\overline{u'w'}$, $\overline{v'w'}$) terms, which were further restricted by removing all estimates where wave contributions made up more than 50% of the total energy. Estimates of $\overline{u'w'}$ and $\overline{u'v'}$ were used to calculate the local Reynolds stress (τ_{RS}) and shear production (P), defined as $\tau_{RS} = \rho\left[\overline{u'w'}^2 + \overline{v'w'}^2\right]^{1/2}$ and $P = \overline{u'w'}\frac{d\overline{U}}{dz} + \overline{v'w'}\frac{d\overline{V}}{dz}$, where $\frac{d\overline{U}}{dz}$ and $\frac{d\overline{V}}{dz}$ are the estimated reef-parallel and cross-channel vertical velocity gradients and ρ is the water density.

Turbulent kinetic energy dissipation rates (ϵ) above and within the oyster reef canopy were calculated using a wave-corrected second order structure function. Best-fit dissipation rates were estimated following a least-squares approach as outlined in Scannell et al. (2017), with second order structure functions computed using vertical velocity time series measured simultaneously within the constant-noise portion of the velocity profile (i.e. 5 cm from probe ± 7 mm). Doppler noise coefficients were estimated from vertical velocity time series (e.g. Thomas et al., 2017) and fits were conducted using a center differencing scheme (e.g. Wiles et al., 2006). All dissipation fits with adjusted R^2 values less than 80% were considered erroneous and removed from further analysis. Importantly, all turbulence metrics reported herein are measured or centered on the lowest noise portion of the velocity profile, which was positioned at approximately 2 cm above the bottom for within canopy measurements and 9.5 cm above the bottom for above canopy measurements. All hydrodynamic measurements (e.g. velocities, wave heights, channel-to-reef current attenuation, turbulent kinetic energy dissipation, etc.) are compared using 95% bootstrapped confidence intervals computed for the mean of each variable.

2.3.2. Biogeochemistry and oyster canopy characteristics

Statistical analyses for all sediment biogeochemical properties and oyster canopy characteristics were performed in SPSS (version 28.0.0.0). First, each dependent variable was tested for the assumptions of normality (using the Shapiro–Wilk test), homogeneity of variance (using the Levene's test), and sphericity (using the Mauchy's Test of Sphericity). Total C and oyster shell length violated the assumption of normality, which was corrected using a log and square-root transformation, respectively. Total P violated the assumption of sphericity, which was corrected using a Greenhouse–Geisser procedure. Time, treatment (i.e. reference, degraded, restored reefs), and their interaction were tested as predictors of live oyster density, shell length, and canopy height, sediment OM content, and total C, N, and P using a mixed ANOVA where time was the within-subjects (repeated) factor and reef was the between subjects factor. A post-hoc Tukey HSD test was used for pairwise comparisons. For all tests, we set the alpha value to 0.05 and assume that measurements collected in individual quadrats are independent. The 24 month post-restoration data for sediment OM, total C, N, P and extractable NO_3^-, NH_4^+, SRP, and DOC were analyzed with a one-way ANOVA using treatment as the sole predictor variable to determine if properties differed by reef type by the end of the study. In this data set, both total N and extractable NO_3^- were log-transformed to meet the assumption of normality.

3. Results

3.1. Oyster recruitment and reef morphology

Prior to restoration, there were no live oysters or oyster canopy on the restored reef (Table 1). Live oyster density (ρ_o: $F = 10.06$, $p < 0.001$, $df = 3$), shell length (L: $F = 367.47.31$, $p < 0.001$, $df = 3$), and canopy height (h_c: $F = 4.84$, $p = 0.005$, $df = 3$) each had significant time*reef interactions. Although no oysters recruited to the restored reef within 1 month of restoration, oyster density estimates at 6 months documented reef colonization, with large numbers of small oysters attached to the recently deployed shell (733.6 ± 67.2 oysters/m^2). These juvenile oysters grew significantly ($p < 0.001$) between 6 (L: 24.7 ± 3.1 mm) and 12 months (47.0 ± 2.1 mm), and mean shell lengths and live oyster densities were not statistically different ($p \geq 0.05$) at the reference and restored reefs for all measurements collected after 1 year. Comparable trends were also

Table 1
Reference and restored reef characteristics. Measurements (mean ± SE) include live oyster density (oysters/m^2), canopy height (mm), and shell length (mm). No live oysters were present on the restored reef before restoration, which occurred in June 2018. The degraded reef, which is not included in the table, did not contain live oyster or canopy structure throughout the study. Canopy height at 1 month post-restoration on the restored reef is indicative of vertically oriented shells on deployed oyster mats.

Reef	Time since restoration	Oyster density (oysters/m^2)	Canopy height (mm)	Shell length (mm)
Restored	1 month	0	33.2 ± 3.5	0
	6 months	733.6 ± 67.2	62.4 ± 4.0	24.7 ± 3.1
	12 months	326.4 ± 57.2	75.6 ± 6.3	47.0 ± 2.1
	30 months	429.6 ± 77.2	85.4 ± 3.0	48.8 ± 1.8
Reference	1 month	150.4 ± 28.0	50.2 ± 6.2	42.0 ± 1.4
	6 months	320.0 ± 29.2	74.4 ± 5.7	46.3 ± 2.0
	12 months	184.0 ± 38.0	61.4 ± 4.1	41.8 ± 0.6
	30 months	332.8 ± 32.8	80.2 ± 2.9	43.9 ± 1.9

observed in canopy height, which showed significant ($p < 0.05$) vertical growth at the restored reef between 1 (33.2 ± 3.5 mm) and 6 months (62.4 ± 4.0 mm) and between 12 (61.4 ± 4.1 mm) and 30 months (80.2 ± 2.9 mm). Mean canopy heights of restored and reference reefs were not statistically different after 1 month post-restoration ($p > 0.05$). Temporal trends in live oyster densities exhibited seasonal variations in recruitment, with significantly ($p < 0.001$) larger oyster densities during the fall high water season (i.e. 6 and 30 months) compared to summer low water season (i.e. 1 and 12 months). This agrees well with recent surveys of oyster spatfall distributions in Mosquito Lagoon, which highlight recruitment cycles with peaks (>750 recruits/m^2) during the late summer and early fall (July–September) and negligible recruitment over the winter and early spring (December–April); Walters et al., 2021a).

Elevation measurements highlight morphological differences between live and degraded reefs, as well as temporal changes at the restored study site (Fig. 2). The degraded reef was steep and unstable (~1 m/yr migration rate: Garvis et al., 2015), with a narrow (<3 m width) reef crest positioned nearly 30 cm above the NAVD-88 datum. Crest elevations at the degraded reef were much higher than the mean high-water level and the surface of the reef was rarely inundated, effectively preventing successful oyster recruitment and cross-reef flow. By contrast, the crest of the reference reef was fully inundated at high tide during all sampling periods. The reference reef was wider than either the degraded or restored reefs, with an oyster-inhabited terrace (> 10 m width) that transitioned sharply along the reef fringe into a wider off-reef plateau. During restoration, crest elevations at the restored reef were reduced by ~20 cm through manual grading (Fig. 2b). The displaced sediments were raked to the seaward edge of the reef, leading to a net elevation gain within ~10 m of the reef crest. Elevation profiles at the restored reef continued to change over the course of the study, with accretion on the reef crest and reworking/scour of sediments along the channel-reef margin. Bed elevations increased by an average of 2.7 cm within the restoration footprint (area: 93.6 m^2) between 1 and 30 months post-restoration, with nearly 10 cm of accretion at the leading edge of the restored reef.

3.2. Reef hydrodynamics

Depth-integrated channel velocities varied over the tidal cycle, with maximum current speeds of 20–30 cm/s observed during peak tidal exchange (Fig. 3). The reference reef canopy was fully submerged to at least 20 cm during all deployments while the crest of the degraded reef was only submerged once during the 30 month experiment. On-reef current velocities were lower than in the channel, highlighting the flow attenuating effects of the reefs.

Near-bed, within-canopy current speeds ranged from 1 to 5 cm/s (Fig. 3e,f), with channel-to-reef current attenuation rates ranging between 88 and 98% (Fig. 4a–c). Near-bed flows on the surface of the degraded and pre-restoration reefs were completely decoupled from those observed in the main channel. At degraded reefs, waves and tidal currents were deflected across the emergent reef crest (a zero-flux boundary), driving irregular, directionally sporadic (±180°) flow patterns (Fig. 5a,b). Although reef- and channel-measured velocities were uncorrelated prior to restoration, lowering of the reef crest re-established over-reef flow resulting in predictable, directionally consistent (±15°) currents similar to those observed at the reference reef (Fig. 5b,c). Mean channel-to-reef velocity attenuation was not statistically different between the restored (mean ± 95% CI: 88.1 ± 2.0%) and reference (89.2 ± 1.3%) reefs within 1 month of restoration. Continued canopy growth increased the attenuation rate at the restored reef to 97.5% within 1 year. Above-canopy velocities (mean: 6.8 ± 0.2 cm/s; max: 10 cm/s) were greater than those measured within the

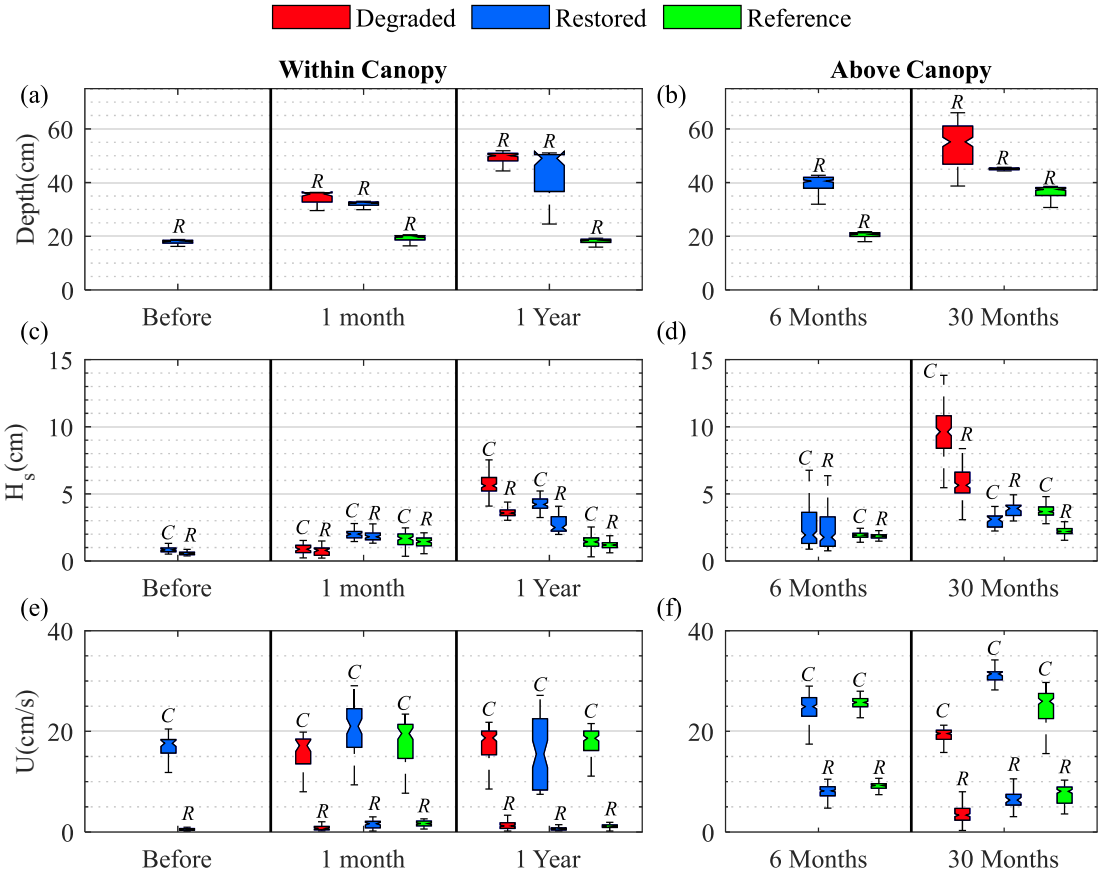

Fig. 3. Distributions of water depths (a, b), wave heights (c, d), and current speeds (e, f) observed within and above canopies of study reefs (red; degraded; blue: restored; green: reference). Current speeds (U) and wave heights (H_s) include paired measurements collected in the channel (*C*) and reef (*R*), while depth measurements were co-located with the velocity profiler on the reef surface. Notches in boxplots represent 95% CI on sample medians.

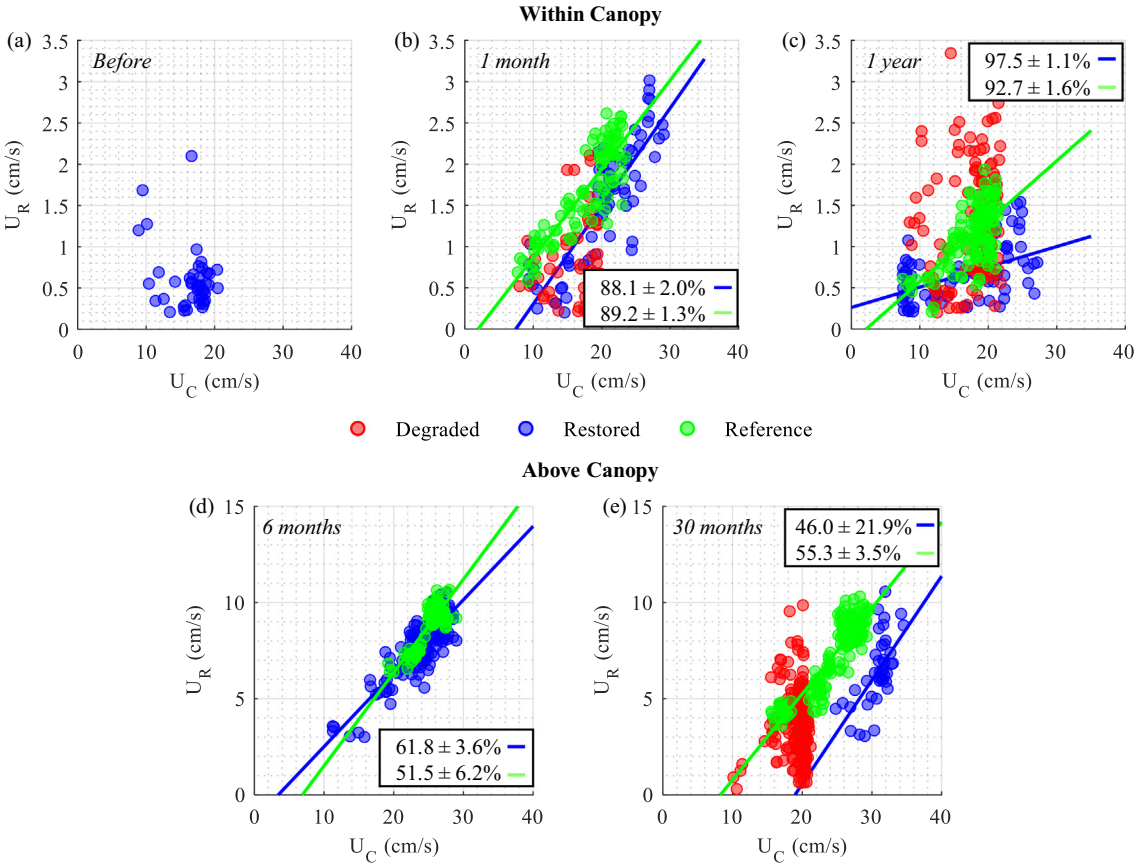

Fig. 4. Channel-to-reef velocity attenuation measured within the canopy near the bed (a, b, c) and above the oyster canopy (d, e). Individual measurements are shown as colored points (red: degraded; blue: restored; green: reference), while best-fit attenuation rates are indicated with lines and colored text. Attenuation rates are only shown for fits with slopes that were significant at the 95% confidence level.

canopy near the bed (mean: 1.1 ± 0.1 cm/s; max 5 cm/s). Increased distance from the boundary and reductions in oyster-cluster interactions led to decreased channel-to-reef current attenuation above the canopy, with estimates between 46% and 62%. Mean above-canopy attenuation rates did not change substantially with time (6 months–30 months) on the reference (51.5 ± 6.2% to 55.3 ± 3.5%) or restored reef (61.8 ± 3.6% to 46.0 ± 21.9%), suggesting that the increase in canopy height observed on the restored reef was not highly influential to flow attenuation above the canopy.

Wave conditions were similar across sample sites (significant wave heights less than 10 cm) and wave heights were generally smaller on the reef than in the main channel (respective means of 2.6 cm and 3.5 cm; Fig. 3c, d). Channel-to-reef wave attenuation rates varied across experiments (−5%–50%), but they were not linked to restoration age or oyster canopy characteristics. Variations were instead most strongly linked to the incoming wave amplitude, wavelength, and on-reef water depth, which are used to characterize wave shoaling and breaking behavior (e.g. Dean and Dalrymple, 1991). Surface waves with large wave heights and wavelengths were more strongly attenuated as they interacted with the reef crest, and attenuation rates were highest when the ratio of wave height and water depth was large. Although a full analysis of the wave behavior is beyond the scope of this study, these results suggest that the wave attenuating capacity of intertidal oyster reefs is more strongly tied to the crest elevation, water depth, and wave climate than to the oyster density or reef condition (e.g. reference, restored, or degraded).

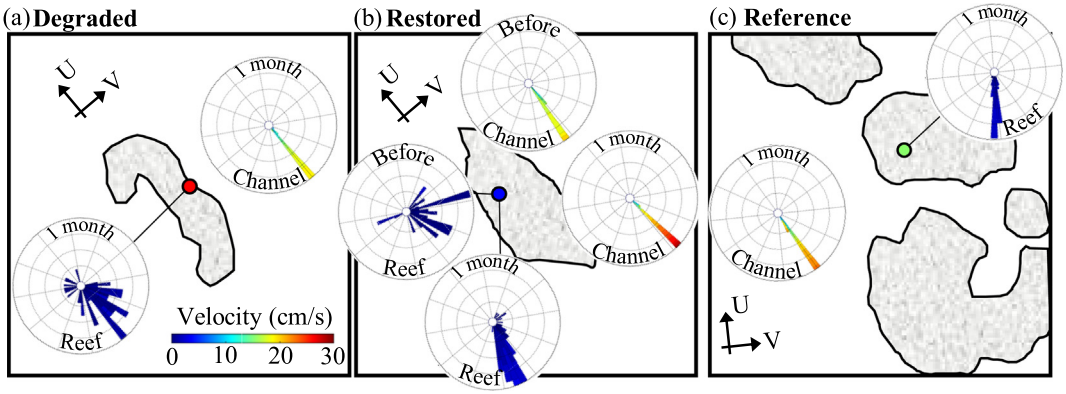

Fig. 5. Near-bed current directionality as observed at the degraded (a), reference (c), and restored (b; pre- and post-restoration) reefs. Current magnitude is indicated with a colormap in (a), while the frequency of velocities observed in each direction band is indicated by the length of the band.

The magnitude of observed turbulence characteristics, including turbulent energy ($\overline{w'^2}$), turbulent kinetic energy dissipation (ϵ), and shear production (P), varied by several orders of magnitude over the course of the study. Turbulence levels generally scaled with the local velocity (U_R), such that the strongest mixing conditions were associated with the fastest flow speeds. Average turbulence rates were highest above the oyster canopy, where $\overline{w'^2}$ was ~10^{-4} m^2/s^2 and ϵ and P ranged from 10^{-6}–10^{-4} m^2/s^3. Flow speeds were lower near the bed, resulting in order of magnitude decreases in all turbulence parameters ($\overline{w'^2}$: 10^{-5} m^2/s^2; ϵ, P: 10^{-7}–10^{-6} m^2/s^3). Observations agreed well with previous reports of mixing within and above the canopies of intertidal oyster reefs (Styles, 2015; Kitsikoudis et al., 2020) and other rigid biological canopies (coral: Reidenbach et al., 2006; mangrove prop roots: Kibler et al., 2019).

When normalized by the local current speed (U_R), turbulence characteristics at the restored and reference reefs (Fig. 6) were similar. Immediately following restoration, normalized turbulent energy ($\overline{w'^2}/U_R^2$) and turbulent kinetic energy dissipation (ϵ/U_R^3) within the canopy at restored and reference reefs were O[10^{-1}] and O[10^{0}] m^{-1}, respectively. Moderate increases in turbulence levels observed between 1 and 12 months coincide with increases in oyster densities measured in both reefs over the same period. Estimates above the canopies of restored and reference reefs also indicated strong agreement, although decreased bed and oyster cluster interactions led to significant reductions in both $\overline{w'^2}/U_R^2$ (O[10^{-2}]) and ϵ/U_R^3 (O[10^{-2}] m^{-1}). There was almost no change to normalized turbulence characteristics above the canopy between 6 and 30 months, reflecting similarities in reef height measured between experiments (Table 1). Shear production was greater than dissipation for all experiments, with P/ϵ ratios in excess of unity both above the canopy and near the bed ($2 < \overline{P/\epsilon} < 5$). P/ϵ ratios were generally larger above the canopy, where mean P/ϵ estimates ranged from 4.2 to 5.0 at the reference reef and 1.9 to 2.5 at the restored reef.

3.3. Sediment biogeochemistry

Organic matter (OM) content of reef sediments varied with time ($F = 5.19$, $p = 0.006$, $df = 3$) and reef type (i.e. reference, restored, degraded; $F = 4.56$, $p = 0.043$, $df = 2$) (Table 2). Specifically, sediment OM (0–5 cm) ranged from 50.2–130.6 g/kg and was higher on all reefs at 12 months, compared to 1 and 6 months post-restoration. Over the entire study period, the reference reef had greater OM content (mean ± standard error; 92.5 ± 18.1 g/kg) than the degraded reef (77.2 ± 6.1 g/kg), while the restored reef had intermediate OM content (80.2 ± 3.9 g/kg). Total carbon (TC) had a significant time*reef interaction ($F = 27.1$, $p < 0.001$; $df = 6$), with degraded reefs having more TC than the reference and restored reefs during the 1-month (87.5 ± 4.5 and 50.1 ± 10.8 g/kg, respectively) and 24-month (95.2 ± 25.0 and 33.0 ± 6.0 g/kg, respectively) samplings. Sediment total nitrogen (TN) generally increased on all reefs over time, from 1.02 ± 0.12 g/kg 1-month post-restoration to 1.82 ± 0.18 g/kg at 24-months post-restoration with a significant time*reef interaction ($F = 11.7$, $p < 0.001$, $df = 6$). TN was generally greater on the reference reef than the degraded reef. Sediment total phosphorous (TP) had a time*reef interaction ($F = 3.49$, $p = 0.018$, $df = 2.64$) and was higher on the reference reef (0.81 ± 0.07 g/kg) than the degraded reef (0.57 ± 0.20 g/kg) at all time points, while the restored reef generally had intermediate TP concentrations (0.66 ± 0.06 g/kg).

Near the end of study period (24 months post-restoration; Table 2), the restored reef had higher extractable DOC (160.1 ± 32.7 mg/kg) than the degraded reef (51.9 ± 8.7 g/kg; $p = 0.02$), while extractable NO_3^-, NH_4^+, and SRP were more highly variable at all study sites (i.e. 1.6 to 4.3 mg NO_3^-/kg, below detection to 19.3 mg NH_4^+/kg, and below detection to 1.7 mg SRP/kg). Although high within-treatment variability limited the statistical significance of between-reef comparisons, the highest concentrations of extractable NH_4^+ were observed on the restored and reference reefs.

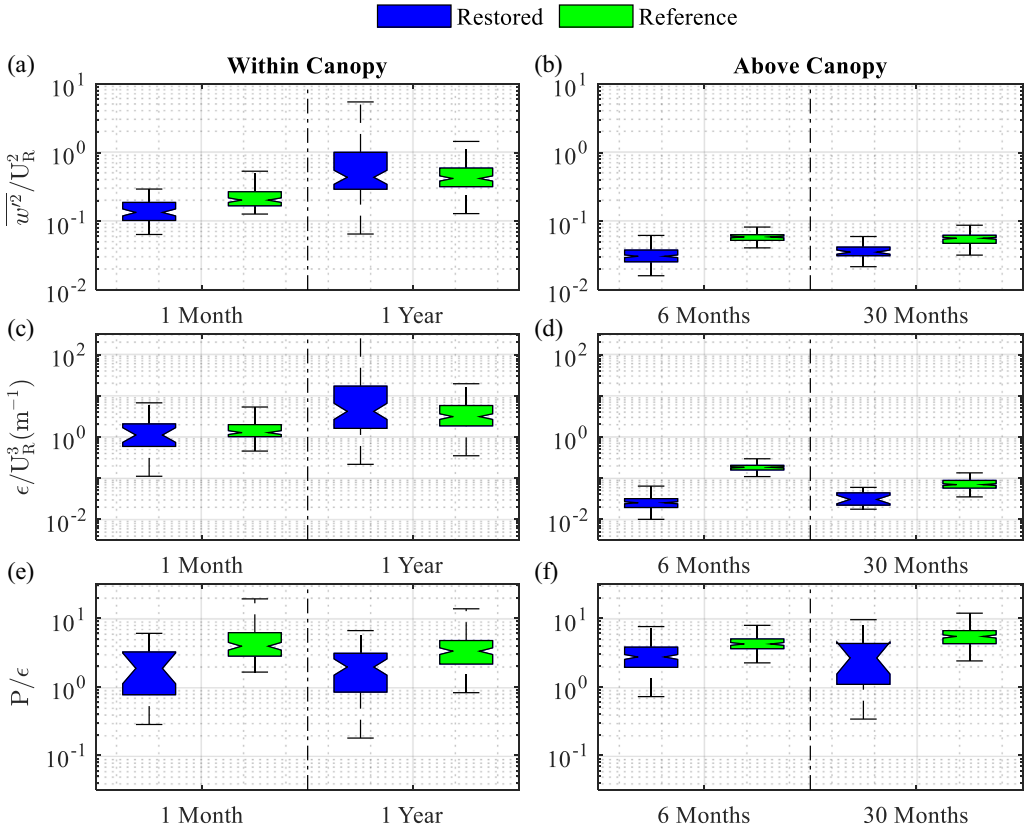

Fig. 6. Normalized turbulence characteristics observed within (a,c,e) and above the canopy (b,d,f) on reference (green) and restored (blue) reefs. Vertical turbulent energy ($\overline{w'^2}$: a–b) and turbulent kinetic energy dissipation (ϵ: c–d) are normalized by the on-reef velocity (U_R), while turbulent production (P: e–f) is normalized by dissipation.

Table 2
Summary of biogeochemical data (mean ± SE) collected on each reef. Phosphorous (P), nitrogen (N), carbon (C), and organic matter (OM) content were analyzed at 1, 6, 12, and 24 months post-restoration, while nitrate (NO_3^-), ammonium (NH_4^+), soluble reactive phosphorous (SRP), and dissolved organic content (DOC) were only analyzed at 24 months post-restoration.

Reef	Time months	P g/kg	C g/kg	N g/kg	OM g/kg	NO_3^- mg/kg	NH_4^+ mg/kg	SRP mg/kg	DOC mg/kg
Degraded	1	0.44 ± 0.02	87.5 ± 2.3	0.49 ± 0.08	60.0 ± 4.3	–	–	–	–
	6	0.68 ± 0.01	30.5 ± 1.1	1.58 ± 0.08	86.1 ± 7.5	–	–	–	–
	12	0.74 ± 0.03	49.4 ± 3.1	1.25 ± 0.08	100.2 ± 2.8	–	–	–	–
	24	0.41 ± 0.14	95.2 ± 12.5	0.99 ± 0.22	62.6 ± 17.1	2.84 ± 0.55	1.78 ± 0.15	0.87 ± 0.37	51.9 ± 8.7
Restored	1	0.67 ± 0.03	42.4 ± 5.1	1.26 ± 0.12	80.2 ± 8.1	–	–	–	–
	6	0.70 ± 0.03	50.7 ± 3.3	1.54 ± 0.04	72.0 ± 3.3	–	–	–	–
	12	0.63 ± 0.02	39.4 ± 2.7	1.51 ± 0.06	97.5 ± 6.0	–	–	–	–
	24	0.63 ± 0.05	30.9 ± 2.4	1.55 ± 0.17	71.0 ± 6.5	1.73 ± 0.08	8.07 ± 4.16	0.46 ± 0.16	160.1 ± 32.7
Reference	1	0.75 ± 0.02	57.9 ± 1.6	1.32 ± 0.06	86.5 ± 2.0	–	–	–	–
	6	0.86 ± 0.05	25.8 ± 1.8	1.19 ± 0.07	78.0 ± 2.4	–	–	–	–
	12	0.84 ± 0.03	33.4 ± 1.6	1.76 ± 0.18	100.3 ± 9.4	–	–	–	–
	24	0.80 ± 0.02	35.2 ± 3.5	2.33 ± 0.26	105.0 ± 12.6	2.65 ± 0.38	10.1 ± 1.96	0.19 ± 0.12	121.1 ± 14.8

4. Discussion

In this study, restoration of an intertidal oyster reef led to notable changes in reef morphology, biogeochemistry, and hydrodynamics. Although the sample size and potentially high reef-to-reef variability (e.g. Chambers et al., 2018) may limit the generic applicability of this study, insight from these results can still be applied to improve reef restoration design and monitoring as well as suggest strategies for successful creation of new intertidal reef. Many of the observed changes occurred immediately following restoration (i.e. within 1 month) before oysters recruited to the reef, as manual lowering of the reef crest facilitated over-reef flow and duration of inundation sufficient to recruit and to sustain growth of recruited oysters. Between 1 and 6 months, large increases in oyster densities and doubling of the canopy height drove enhanced sequestration and burial of organic material at the sediment surface, increasing sediment extractable nutrients (e.g. DOC, NH_4^+, etc.). Below, we integrate the canopy, hydrodynamic, and biogeochemical results of the study to discuss (1) the evolution of reef elevation profiles and canopy characteristics and their influence on local hydrodynamics; (2) the effects of reef hydrodynamics and oyster recruitment on sediment biogeochemistry; and (3) the evolution of physical and biogeochemical properties on the restored reef as a function of time since restoration.

4.1. Initial elevation grading and canopy evolution influence local reef hydrodynamics

Reef restoration had an immediate and profound impact on flow patterns observed on the surface of the restored reef. Flow patterns shifted from flashy and directionally sporadic (i.e. similar to the degraded reef) to tidally driven and unidirectional (i.e. similar to the reference reef) immediately following restoration, when the reef crest was manually lowered to restore periodic inundation at the site. The restoration of over-reef flow increased channel-to-reef connectivity and promoted successful oyster recruitment, which relies on both oyster spat availability and inundation frequency (Ridge et al., 2015). The dramatic pre- to post-restoration shift in flow patterns highlighted the influence of bulk reef structure (e.g. crest elevation relative to water level, reef slope), as opposed to smaller scale canopy characteristics (e.g. oyster density, canopy height), in influencing over-reef flow at the restored reef.

As the canopy evolved over time with recruitment, within-canopy flow characteristics were well correlated with changes in live oyster density, while above-canopy flows were less influenced by oyster characteristics. In the canopy of the restored reef, channel-to-reef velocity attenuation rates increased by nearly 10% between 1 (88.1%) and 12 (97.5%) months, while average normalized vertical turbulent energy ($\overline{w'^2}/U_R^2$) and dissipation (ϵ/U_R^3) increased by 225% and 275%, respectively. Over this same period, live oyster densities grew from 0 to 326.4 oysters/m^2, increasing the solid volume fraction of near-bed canopy elements. The increase in structural complexity played a major role in modifying hydrodynamics within the canopy, where turbulence generation was controlled by a combination of bed friction, canopy-element interactions, and downstream turbulence transport (e.g. Monismith, 2007; Davis et al., 2021). This complex turbulence budget was reflected in the imbalance of shear production and dissipation within the canopy ($\overline{P/\epsilon}$: 2–4), as well as the multi-order variability in normalized mixing characteristics near the bed (ϵ/U_R^3: 0.1–100 m^{-1}; $\overline{w'^2}/U_R^2$: 0.001–10). Similar findings of imbalanced turbulence budget have been reported for intertidal oyster reefs in Mosquito Lagoon (Kitsikoudis et al., 2020), where variability was linked to reef heterogeneity, vortex shedding, and turbulent injections from above the canopy surface.

Flow and turbulence characteristics measured above the canopy were nearly constant throughout the study, despite significant changes in canopy height and oyster density. This is somewhat surprising given previous studies above rigid canopies (e.g. Styles, 2015; Reidenbach et al., 2006), which have found that turbulence characteristics are almost entirely controlled by the canopy height (and structure) itself. As water flows across the canopy, a shear layer forms at the canopy-flow interface, attenuating over-reef currents and enhancing turbulent production. The lack of detectable flow changes in the current study may be explained by the measurement position and experimental design. Although canopy heights on the restored reef increased significantly between 6 and 30 months (62 to 85 mm; $p = 0.002$), measurement positions (z) were always located within a few centimeters of the canopy surface (h). For all deployments, estimates of the z/h ratio ($1.2 < z/h < 1.5$) placed the sample volume well within the above-canopy shear layer, where turbulence characteristics are expected to vary little with z/h (e.g. Ghisalberti and Nepf, 2006).

While above-canopy turbulence characteristics were constant with time, normalized turbulence metrics on the restored reef ($\overline{w'^2}/U_R^2$: $3.3 \pm 0.1 \times 10^{-2}$; ϵ/U_R^3: $2.5 \pm 0.2 \times 10^{-2}$ m^{-1}) were consistently lower than those observed on the reference reef ($\overline{w'^2}/U_R^2$: $5.5 \pm 0.2 \times 10^{-2}$; ϵ/U_R^3: $9.4 \pm 0.8 \times 10^{-2}$ m^{-1}). These differences may have significant consequences for sediment transport, nutrient retention, and larval recruitment, which all rely on turbulent mixing for transport. For example, increased turbulence may promote sediment and waste flushing from the reef surface, preventing oyster burial and mortality (e.g. Lenihan, 1999). Variations in turbulence were not readily linked to canopy evolution, since live oyster densities, canopy heights, and shell lengths on the restored reef all matched or exceeded those observed on the reference reef within 1 year of restoration. As previously discussed, mixing above the canopy is strongly related to the effective "roughness" of the canopy structure (i.e. Reidenbach et al., 2006), which varies as a complex function of the canopy height, the canopy element density, and the total reef area. Although the canopy characteristics presented herein were sufficient for assessing reef health and canopy growth, they may have been too coarse (spatially) to describe

the reef-scale roughness relevant for above canopy turbulence generation. Another possibility is that the size of the study reefs (reference: ~500 m^2; restored: ~100 m^2) may have differentially affected shear layer development at the site, with a more persistent above canopy shear layer developing at the reference reef where the over-reef flow path was longer. These results highlight the need for additional studies focused on parameterizing turbulent flow above intertidal oyster reefs.

4.2. Hydrodynamics and oyster recruitment promote accretion and change sediment biogeochemistry

Physical and biological processes in the canopy acted together to reshape the restored reef over the study period, raising the crest elevation and steepening the leading edge of the restored reef as it actively evolved toward reference conditions. The net sediment accretion observed on the restored reef surface 30 months after restoration reflects coupled physical and biological controls on sediment transport dynamics within the canopy. Oysters increase the flux of suspended particulate matter from the overlying water to the bed through active filtration (e.g. Locher et al., 2020; Wildish and Kristmanson, 1997). Particles are deposited on the bed as feces and pseudofeces, where they form a layer of unconsolidated, carbon-rich biodeposits (e.g. Haven and Morales-Alamo, 1966). The canopy also exerts hydrodynamic controls on suspended sediments, which may settle out of the water column as flow is attenuated through the complex reef structure (e.g. Reidenbach et al., 2013). Here, canopy growth was directly correlated with enhanced current attenuation between 1 and 12 months post-restoration, providing some of the first direct evidence of canopy growth reducing near-bed velocities and promoting passive particle settling.

Oyster-mediated sediment and waste (i.e. feces and pseudofeces) deposition had a pronounced effect on sediment biogeochemistry. In general, functional oyster canopies are expected to enhance the sequestration and burial of organic material at the sediment surface, altering the nutrient and microbial community composition of benthic soils (e.g. Kellogg et al., 2013). The small sample size and high within-treatment variability of the current study limited the ability to adequately test the hypothesis that the tandem development of the reef structure and oyster recruitment results in enhanced benthic-pelagic coupling, increasing the cycling and storage of total sediment N and P, as has been shown in previously in this region (Chambers et al., 2018). However, the elevated concentrations of extractable DOC and NH_4^+ found at the 24-month sampling in the restored reef sediments do suggest a shift toward biogeochemical properties more closely resembling the reference reef. These two labile nutrients (i.e. DOC, NH_4^+) are among the first sediment nutrient pools to respond to oyster recruitment following restoration, can be a direct consequence of the deposition of oyster feces and pseudofeces, and are particularly enriched within the biodeposition of juvenile (<14 months) oysters (Locher et al., 2020). This finding suggests the sediment of the restored and reference reefs are an organic-enriched environment relative to the degraded reef, which may not be readily apparent when quantifying only total C pools because of the inclusion of carbonate C of disarticulated oyster shells (Hurst et al., in review).

4.3. Applying the restoration trajectory to reef design and monitoring

The restoration trajectory observed in this study (immediate shift in reef flow patterns followed by gradual changes in near-bed flow and sediment characteristics associated with the developing oyster canopy) may offer insight to planning successful future reef restorations. Whether restoring historic reef footprints or creating new reef, results of this study highlight the vital influence of establishing hydraulic connectivity across restored or created reef and demonstrate how hydrology facilitates recruitment and development of the oyster canopy. The evolution of ecosystem services on restored reef can be broadly framed as a two-part development trajectory model (e.g. Craft et al., 2003; van Andel and Aronson, 2012; La Peyre et al., 2014). Temporal changes are linked to either (1) site preparation, including change to reef/bed elevation and the addition of hard structure, or (2) living oyster populations, where services developed over time with increasing oyster densities. This model is similar to that proposed for oyster reefs created using mounded aggregate (La Peyre et al., 2014), with the notable addition of trajectories associated with elevation changes. Below, we highlight the temporal changes associated with each trajectory, expanding the framework to include restoration related changes observed both in this and other restoration studies, and specify how these observations can be applied to improve restoration design and monitoring strategies.

During site preparation, reefs may be manually graded to lower the crest below the mean high-water level (as described herein) or material may be placed on the bed to create the bulk reef structure (e.g. Piazza et al., 2005; Scyphers et al., 2011; La Peyre et al., 2014). Whether restoration site preparations entail lowering or raising bed elevation, establishing appropriate hydrodynamic function in terms of frequency, depth and duration of crest inundation is a vital aspect of successful intertidal reef design. Intertidal *C. virginica* requires full inundation well over 50% of the time (Morris et al., 2021). Establishing the appropriate reef elevations to allow sufficient inundation over the tidal cycle produces flow patterns and channel-to-reef connectivity needed for oyster recruitment and sustained growth. However, created oyster reef may be designed to satisfy multiple objectives, including coastal stabilization (Morris et al., 2019), thus wave or current attenuation may be a relevant reef design parameter related to crest elevation. As hydrodynamic attenuation tends to increase as water level over the reef decreases (Spiering et al., 2021; Wiberg et al., 2019), reef designers may feel opposing pressures to thread the needle of establishing reef elevations high enough to attain flow attenuation objectives, but low enough to maintain recruitment and growth of oyster (Morris et al., 2021). The results of this study clearly demonstrate the importance of establishing design elevations that promote hydrodynamic connectivity across the reef, ideally informed by pre-installation monitoring or modeling of water level variability at the site. The early hydrodynamic impact and connection to later recruitment success demonstrated in this study also suggest that reef impact monitoring should begin immediately after restoration or reef creation. For instance, immediately establishing over-reef depth monitoring during low and high tide or duration of crest inundation could point to early problems in the restoration design that could eventually hinder recruitment success.

Longer-term monitoring should include the more traditional measurement of recruitment and canopy development, as many of the most ecologically significant transformations on restored oyster reefs occur as a direct result of oyster recruitment, with associated physical and biogeochemical changes occurring over oyster population timescales. From a physical standpoint, oyster recruitment and canopy growth enhance current and wave attenuation (this study, Manis et al., 2014; Whitman and Reidenbach, 2012) while mechanically stabilizing the bed (Scyphers et al., 2011) and promoting accretion through enhanced particle trapping capacity (this study, Newell et al., 2005). This prevents reef erosion, which in turn protects the shoreline and maintains crest elevations at the inundation depth required for oyster proliferation. Increased oyster densities also act to enhance mixing near the bed, as reported in the current study, which is crucial for periodically flushing feces and pseudofeces and preventing the suffocation of oysters at the base of the canopy (e.g. Lenihan, 1999). From a biogeochemical perspective, young oysters (<12 months) remove chlorophyll-a more rapidly than older oysters, contributing to high concentrations of DOC, NO_3^-, and NH_4^+ in their feces and pseudo-feces (Locher et al., 2020). As live oyster densities grow, total filtration rates increase (La Peyre et al., 2014; Galimany et al., 2017) and organic carbon and nutrient storage is enhanced (Chambers et al., 2018). Canopy structures created by living oysters also enhance habitat complexity, increasing the abundance of prey and predator species that utilize the reef for refuge and feeding (e.g. Peterson et al., 2003).

Ecosystem services are limited by the recruitment and survival of oyster populations on restored reefs. Service provision occurs over time as oyster densities increase, with a rate of change related to local oyster recruitment and growth rates (e.g. La Peyre et al., 2014). As oyster densities approach

sustainable population levels and growth slows or stops, ecosystem services plateau at levels similar to reference reefs. Under ideal conditions (e.g. high larval density and food availability, appropriate restoration technique) canopy heights and live oyster densities on restored reefs can display promising trajectories toward reference conditions within a single year, especially in subtropical estuaries with extended recruitment seasons. This is the case in the current study area (i.e. Mosquito Lagoon, FL, USA), where rapid oyster recruitment is at least partially linked to the extended growing season (April through December; L. Walters pers. obs.). Reef restoration projects in areas with less ideal environmental conditions will likely see slower changes (3–5 years), as evidenced by work in less productive systems where resident oyster populations are smaller (e.g. La Peyre et al., 2014; Schulte and Burke, 2014). In general, the strong link between oyster populations and ecosystem service provision suggests that a post-restoration focus on live oyster density monitoring may be a sufficient proxy for characterizing the "success" of restoration on several ecological functions, from energy attenuation to the promoting of biogeochemical cycling.

5. Conclusion

In this study, a degraded intertidal oyster reef was restored and monitored for nearly three years (30 months). Pre- and post-restoration changes in canopy, hydrodynamics and biogeochemistry were compared to conditions on nearby live reference and degraded reefs. This work was designed as a case study to determine the time required for a reef restored using elevation grading to behave similarly to live intact reefs, as well as to investigate linkages between physical, biological, and chemical changes on a restored reef. Although the sample size was low (by design) and conclusions may not be applicable for all reef restoration projects, the results presented herein provide valuable insights for the evolution of restored oyster reefs and may inform future experimental designs. Periodic inundation and over-reef flow on the restored reef were reestablished immediately following restoration when the reef crest was lowered and stabilized. Favorable growing conditions allowed rapid oyster recruitment and growth on deployed oyster shell mats, and live oyster densities, shell lengths, and canopy heights were not statistically different than those observed on a reference reef within 12 months of restoration. Increased oyster densities were linked to enhanced mixing and velocity attenuation within the canopy, and near-bed turbulence and mean flow characteristics were not statistically different from reference conditions within 12 months. Measurements above the canopy showed that normalized turbulence characteristics were consistently weaker on the restored reef compared to the reference reef, with minor differences potentially linked to variations in bulk reef morphology. Sediment nutrient pools (total carbon, total nitrogen) on restored and reference reefs were also comparable within 12 months, and changes in nutrients and organic carbon were linked to increases in oyster density over the same period. Net sediment accretion was observed on the surface of the restored reef over the course of the study, suggesting that the oyster canopy retained sediments through deposition of oyster biodeposits and by promoting deposition of suspended sediments as flows were attenuated within the canopy. Results were used to describe a two-part restoration trajectory model for degraded reefs requiring changes in bed elevation, where changes related to site preparation occur immediately following restoration and changes related to oyster populations occur over time as living oyster densities increase at the site, with development timescales set by local site conditions (i.e. established reproductive oyster populations, climate, etc.). This study shows that if oyster recruitment and survival is successful, the impact of reef restoration can be realized quickly, and restored intertidal oyster reefs can recover rapidly (within 1 year) with a promising trajectory toward conditions on natural reefs.

CRediT authorship contribution statement

David Cannon: Methodology, Formal Analysis, Investigation, Data Curation, Writing - Original Draft, Writing – Review & Editing, Visualization. **Kelly Kibler:** Conceptualization, Methodology, Investigation, Writing – Review & Editing, Supervision, Funding Acquisition. **Linda Walters:** Conceptualization, Methodology, Formal Analysis, Investigation, Writing - Original Draft, Writing – Review & Editing, Funding Acquisition. **Lisa Chambers:** Conceptualization, Methodology, Formal Analysis, Investigation, Writing - Original Draft, Writing – Review & Editing, Funding Acquisition.

Declaration of competing interest

The authors declare that they have no known competing financial interests or personal relationships that could have appeared to influence the work reported in this paper.

Acknowledgments

This research was funded by the U.S. National Science Foundation (NSF grants #1944880 and #1617374), the Indian River Lagoon National Estuary Program, and the University of Central Florida. In-kind support was provided by the National Park Service at Canaveral National Seashore. The authors would also like to thank all volunteers for their work restoring oyster reefs in Mosquito Lagoon. Additionally, the authors thank V. Kitsikoudis, D. Spiering, P. Sacks and numerous UCF students for assistance with data collection.

References

van Andel, J., Aronson, J., 2012. Restoration Ecology: The New Frontier. Wiley-Blackwell.
Andersen, J.M., 1976. An ignition method for determination of total phosphorus in lake sediments. Water Res. 10, 329–331. https://doi.org/10.1016/0043-1354(76)90175-5.
Barnes, T.K., Volety, A.K., Chartier, K., Mazzotti, F.J., Pearlstine, L., 2007. A habitat suitability index model for the eastern oyster (Crassostrea virginica), a tool for restoration of the Caloosahatchee Estuary, Florida. J. Shellfish Res. 26, 949–959. https://doi.org/10.2983/0730.
Beck, M.W., Brumbaugh, R.D., Airoldi, L., Carranza, A., Coen, L.D., Crawford, C.O., et al., 2011. Oyster reefs at risk and recommendations for conservation, restoration, and management. Bioscience 61, 107–116. https://doi.org/10.1525/bio.2011.61.2.5.
Blomberg, B.N., Pollack, J.B., Montagna, P.A., Yoskowitz, D.W., 2018. Evaluating the U.S. Estuary restoration act to inform restoration policy implementation: a case study focusing on oyster reef projects. Mar. Policy 91, 161–166. https://doi.org/10.1016/J.MARPOL.2018.02.014.
Bricker, J.D., Monismith, S.G., 2007. Spectral wave–turbulence decomposition. J. Atmos. Ocean. Technol. 24, 1479–1487.
Chambers, L.G., Gaspar, S.A., Pilato, C.J., Steinmuller, H.E., McCarthy, K.J., Sacks, P.E., Walters, L.J., 2018. How well do restored intertidal oyster reefs support key biogeochemical properties in a coastal Lagoon? Estuar. Coasts 41, 784–799. https://doi.org/10.1007/s12237-017-0311-5.
Coen, L.D., Luckenbach, M.W., 2000. Developing success criteria and goals for evaluating oyster reef restoration: ecological function or resource exploitation? Ecol. Eng. 15, 323–343. https://doi.org/10.1016/S0925-8574(00)00084-7.
Craft, C., Megonigal, P., Broome, S., Stevenson, J., Freese, R., Cornell, J., Zheng, L., Sacco, J., 2003. The place of ecosystem development of constructed Spartina alterniflora marshes. Ecol. Appl. 13, 1417–1432. https://doi.org/10.1890/02-5086.
Dame, R.F., Spurrier, J.D., Wolaver, T.G., 1989. Carbon, nitrogen, and phosphorous processing by an oyster reef. Mar. Ecol. Prog. Ser. 54, 249–256.
Davis, K.A., Pawlak, G., Monismith, S.G., 2021. Turbulence and coral reefs. Annu. Rev. Mar. Sci. 13. https://doi.org/10.1146/annurev-marine-042120-071823.
Dean, R., Dalrymple, R., 1991. Water Wave Mechanics for Engineers and Scientists2. World Scientific Publishing Company.
Elliott, M., Burdon, D., Hemingway, K.L., Apitz, S.E., 2007. Estuarine, coastal and marine ecosystem restoration: confusing management and science - a revision of concepts. Estuar. Coast. Shelf Sci. 74, 349–366. https://doi.org/10.1016/j.ecss.2007.05.034.
Fodrie, F.J., Rodriguez, A.B., Gittman, R.K., Grabowski, J.H., Lindquist, N.L., Peterson, C.H., Piehler, M.F., Ridge, J.T., 2017. Oyster reefs as carbon sources and sinks. Proc. R. Soc. B Biol. Sci. 284, 20170891. https://doi.org/10.1098/rspb.2017.0891.
Galimany, E., Freeman, C.J., Lunt, J., Domingos, A., Sacks, P., Walters, L.J., 2017. Feeding competition between the native oyster Crassostrea virginica and the invasive mussel mytella charruana. Mar. Ecol. Prog. Ser. 564, 57–66. https://doi.org/10.3354/MEPS11976.
Garvis, S.K., Sacks, P.E., Walters, L.J., 2015. Formation, movement, and restoration of dead intertidal oyster reefs in Canaveral National Seashore and Mosquito Lagoon, Florida. J. Shellfish Res. 34, 251–258. https://doi.org/10.2983/035.034.0206.
Ghisalberti, M., Nepf, H., 2006. The structure of the shear layer in flows over rigid and flexible canopies. Environ. Fluid Mech. 6, 277–301. https://doi.org/10.1007/s10652-006-0002-4.
Goelz, T., Vogt, B., Hartley, T., 2020. Alternative substrates used for oyster reef restoration: a review. J. Shellfish Res. 39, 1–12. https://doi.org/10.2983/035.039.0101.
Goring, D.G., Nikora, V.I., 2002. Despiking acoustic doppler velocimeter data. J. Hydraul. Eng. 128, 117–126. https://doi.org/10.1061/(asce)0733-9429(2002)128:1(117).

Gregalis, K., Powers, S., Heck, K.L., 2008. Restoration of oyster reefs along a bio-physical gradient in Mobile Bay, Alabama. J. Shellfish Res. 27, 1163–1169. https://doi.org/10.2983/0730-8000-27.5.1163.

Grizzle, R.E., Adams, J.R., Walters, L.J., 2002. Historical changes in intertidal oyster (Crassostrea virginica) reefs in a Florida lagoon potentially related to boating activities. J. Shellfish Res. 21, 749–756.

Hansen, J.C.R., Reidenbach, M.A., 2017. Turbulent mixing and fluid transport within Florida Bay seagrass meadows. Adv. Water Resour. 108, 205–215. https://doi.org/10.1016/j.advwatres.2017.08.001.

Haven, D.S., Morales-Alamo, R., 1966. Aspects of biodeposition by oysters and other invertebrate filter feeders. Limnol. Oceanogr. 11, 487–498. https://doi.org/10.4319/LO.1966.11.4.0487.

Hawthorne, T.L., Toohy, K.R., Yang, B., Graham, L., Lorenzo, E.M., Torres, H., et al., 2022. Mapping emotional attachment as a measure of sense of place to identify coastal restoration priority areas. Appl. Geogr. 138, 102608.

Hernández, A.B., Brumbaugh, R.D., Frederick, P., Grizzle, R., Luckenbach, M.W., Peterson, C.H., Angelini, C., 2018. Restoring the eastern oyster: how much progress has been made in 53 years? Front. Ecol. Environ. 16, 463–471. https://doi.org/10.1002/FEE.1935.

Holley, J.R., McComas, K.A., Hare, M.P., 2018. Troubled waters: risk perception and the case of oyster restoration in the closed waters of the Hudson-Raritan estuary. Mar. Policy 91, 104–112. https://doi.org/10.1016/J.MARPOL.2018.01.024.

Hurst et al., in review, N.R. Hurst B. Locher H. E. Steinmuller L. J. Walters L.G. Chambers , in review. Organic carbon dynamics and microbial community response to oyster reef restoration. Limnol. Oceanogr.

Indian River Lagoon National Estuary Program, 2020. Indian River Lagoon Climate Ready Estuary Report.

Kellogg, M.L., Cornwell, J.C., Owens, M.S., Paynter, K.T., 2013. Denitrification and nutrient assimilation on a restored oyster reef. Mar. Ecol. Prog. Ser. 480, 1–19. https://doi.org/10.3354/MEPS10331.

Kennedy, V.S., Newell, R.I.E., Eble, A.F., 1996. The Eastern Oyster: Crassostrea virginica. Maryland Sea Grant College.

Kibler, K.M., Kitsikoudis, V., Donnelly, M., Spiering, D.W., Walters, L., 2019. Flow–vegetation interaction in a living shoreline restoration and potential effect to mangrove recruitment. Sustainability 11, 3215. https://doi.org/10.3390/su11113215.

Kitsikoudis, V., Kibler, K., Walters, L., 2020. In-situ measurements of turbulent flow over intertidal natural and degraded oyster reefs in an estuarine lagoon. Ecol. Eng. (143).

La Peyre, M.K., Humphries, A.T., Casas, S.M., La Peyre, J.F., 2014. Temporal variation in development of ecosystem services from oyster reef restoration. Ecol. Eng. 63, 34–44. https://doi.org/10.1016/J.ECOLENG.2013.12.001.

La Peyre, M., Schwarting, L., Miller, S., 2013. Baseline data for evaluating development trajectory and provision of ecosystem services of created fringing oyster reefs in Vermilion Bay, Louisiana. Open-File Rep. https://doi.org/10.3133/OFR20131053.

Lenihan, H.S., 1999. Physical-biological coupling on oyster reefs: how habitat structure influences individual performance. Ecol. Monogr. 69, 251–275. https://doi.org/10.1890/0012-9615(1999)069[0251:PBCOOR]2.0.CO;2.

Loch, J.M.H., Walters, L.J., Donnelly, M.L., Cook, G.D., 2021. Restored coastal habitat can "Reel in" juvenile sportfish: population and community responses in the Indian River lagoon, Florida, USA. Sustainability 13 (22), 12832. https://doi.org/10.3390/su132212832.

Locher, B., Hurst, N.R., Walters, L.J., Chambers, L.G., 2020. Juvenile oyster (Crassostrea virginica) biodeposits contribute to a rapid rise in sediment nutrients on restored intertidal oyster reefs (Mosquito lagoon, FL, USA). Estuar. Coasts 1–17. https://doi.org/10.1007/s12237-020-00874-2.

Manis, J.E., Garvis, S.K., Jachec, S.M., Walters, L.J., 2014. Wave attenuation experiments over living shorelines over time: a wave tank study to assess recreational boating pressures. J. Coast. Conserv. 191 (19), 1–11. https://doi.org/10.1007/S11852-014-0349-5 2014.

McClenachan, G.M., Donnelly, M.J., Shaffer, M.N., Sacks, P.E., Walters, L.J., 2020. Does size matter? Quantifying the cumulative impact of small-scale living shoreline and oyster reef restoration projects on shoreline erosion. Restor. Ecol. 28, 1365–1371. https://doi.org/10.1111/rec.13235.

Meyer, D.L., Townsend, E.C., Thayer, G.W., 1997. Stabilization and erosion control value of oyster cultch for intertidal marsh. Restor. Ecol. 5, 93–99. https://doi.org/10.1046/j.1526-100X.1997.09710.x.

Monismith, S.G., 2007. Hydrodynamics of coral reefs. Annu. Rev. Fluid Mech. 39, 37–55.

Morris, R.L., Bilkovic, D.M., Boswell, M.K., Bushek, D., Cebrian, J., Goff, J., Kibler, K.M., La Peyre, M.K., McClenachan, G., Moody, J., Sacks, P., 2019. The application of oyster reefs in shoreline protection: are we over-engineering for an ecosystem engineer? J. Appl. Ecol. 56 (7), 1703–1711.

Morris, R.L., La Peyre, M.K., Webb, B.M., Marshall, D.A., Bilkovic, D.M., Cebrian, J., McClenachan, G., Kibler, K.M., Walters, L.J., Bushek, D., Sparks, E.L., 2021. Large-scale variation in wave attenuation of oyster reef living shorelines and the influence of inundation duration. Ecol. Appl. 31 (6), e02382.

Newell, R., Fisher, T., Holyoke, R., Cornwell, J., 2005. Influence of eastern oysters on nitrogen and phosphorous regeneration in Chesapeake Bay, USA. The Comparative Roles of Suspension-Feeders in Ecosystems. Springer, Dordrecht, pp. 93–120.

Nitsch, C.K., Walters, L.J., Sacks, J.S., Sacks, P.E., Chambers, L.G., 2021. Biodegradable material for oyster reef restoration: first-year performance and biogeochemical consideration in a coastal lagoon. 2021Sustainability 13, 7415. https://doi.org/10.3390/SU13137415 13: 7415.

Peterson, C.H., Grabowski, J.H., Powers, S.P., 2003. Estimated enhancement of fish production resulting from restoring oyster reef habitat: quantitative valuation. Mar. Ecol. Prog. Ser. 264, 249–264. https://doi.org/10.3354/MEPS264249.

Phlips, E.J., Badylak, S., Lasi, M.A., 2014. From red tides to green and brown tides: bloom dynamics in a restricted subtropical lagoon under shifting climatic conditions. Estuar. Coasts 383 (38), 886–904. https://doi.org/10.1007/S12237-014-9874-6 2014.

Piazza, B.P., Banks, P.D., La Peyre, M.K., 2005. The potential for created oyster shellreefs as a sustainable shoreline protection strategy in Louisiana. Restor. Ecol. 13, 499–506.

Pine, W.E., Walters, C.J., Camp, E.V., Bouchillon, R., Ahrens, R., Sturmer, L., Berrigan, M.E., 2015. The curious case of eastern oyster Crassostrea virginica stock status in Apalachicola Bay, Florida. Ecol. Soc. 20 (3).

Powers, S.P., Peterson, C.H., Grabowski, J.H., Lenihan, H.S., 2009. Success of constructed oyster reefs in no-harvest sanctuaries: implications for restoration. Mar. Ecol. Prog. Ser. 389, 159–170.

Reidenbach, M.A., Berg, P., Hume, A., Hansen, J.C.R., Whitman, E.R., 2013. Hydrodynamics of intertidal oyster reefs: the influence of boundary layer flow processes on sediment and oxygen exchange. Limnol. Oceanogr. Fluids Environ. 3, 225–239. https://doi.org/10.1215/21573689-2395266.

Reidenbach, M.A., Monismith, S.G., Koseff, J.R., Yahel, G., Genin, A., 2006. Boundary layer turbulence and flow structure over a fringing coral reef. Limnol. Oceanogr. 51, 1956–1968. https://doi.org/10.4319/lo.2006.51.5.1956.

Ridge, J.T., Rodriguez, A.B., Fodrie, F.J., Lindquist, N.L., Brodeur, M.C., Coleman, S.E., Grabowski, J.H., Theuerkauf, E.J., 2015. Maximizing oyster-reef growth supports green infrastructure with accelerating sea-level rise. Sci. Rep. 5, 14785. https://doi.org/10.1038/srep14785.

Rodriguez, A.B., Fodrie, F.J., Ridge, J.T., et al., 2014. Oyster reefs can outpace sea-level rise. Nat. Clim. Chang. 4, 493–497.

Scannell, B.D., Rippeth, T.P., Simpson, J.H., Polton, J.A., Hopkins, J.E., 2017. Correcting surface wave bias in structure function estimates of turbulent kinetic energy dissipation rate. J. Atmos. Ocean. Technol. 34, 2257–2273. https://doi.org/10.1175/JTECH-D-17-0059.1.

Schulte, D., Burke, R., 2014. Recruitment enhancement as an indicator of oyster restoration success in Chesapeake Bay. Ecol. Restor. 32 (4), 434–440.

Schulte, D.M., Burke, R.P., Lipcius, R.N., 2009. Unprecedented restoration of a native oyster metapopulation. Science 325, 1124–1128. https://doi.org/10.1126/SCIENCE.1176516.

Scyphers, S.B., Powers, S.P., Heck Jr., K.L., Byron, D., 2011. Oyster reefs as natural breakwaters mitigate shoreline loss and facilitate fisheries. PLoS One 6, e22396. https://doi.org/10.1371/JOURNAL.PONE.0022396.

Smith, N., 1993. Tidal and wind-driven transport between Indian River and Mosquito Lagoon, Florida. Florida Sci. 56 (4), 235–246.

Spiering, D.W., Kibler, K.M., Kitsikoudis, V., Donnelly, M.J., Walters, L.J., 2021. Detecting hydrodynamic changes after living shoreline restoration and through an extreme event using a before-after-control-impact experiment. Ecol. Eng. 169, 106306.

Steward, J.S., Virnstein, R.W., Lasi, M.A., Morris, L.J., Miller, J.D., Hall, L.M., Tweedale, W.A., 2006. The impacts of the 2004 hurricanes on hydrology, water quality, and seagrass in the Central Indian River Lagoon, Florida. Estuar. Coasts 296 (29), 954–965. https://doi.org/10.1007/BF02798656 2006.

Styles, R., 2015. Flow and turbulence over an oyster reef. J. Coast. Res. 31, 978–985. https://doi.org/10.2112/JCOASTRES-D-14-00115.1.

Theuerkauf, S.J., Lipcius, R.N., 2016. Quantitative validation of a habitat suitability index for oyster restoration. Front. Mar. Sci., 64 https://doi.org/10.3389/FMARS.2016.00064.

Theuerkauf, S.J., Eggleston, D.B., Puckett, B.J., 2019. Integrating ecosystem services considerations within a GIS-based habitat suitability index for oyster restoration. PLoS One 14 (1), e0210936.

Thomas, R.E., Schindfessel, L., McLelland, S.J., Creëlle, S., De Mulder, T., 2017. Bias in mean velocities and noise in variances and covariances measured using a multistatic acoustic profiler: the nortek vectrino profiler. Meas. Sci. Technol. 28, 075302. https://doi.org/10.1088/1361-6501/aa7273.

USEPA, 1993. Methods for the Determination of Inorganic Substances in Environmental Samples. EPA/600/R-933/100.

Wahl, T., 2003. Discussion of "Despiking acoustic doppler velocimeter data" by Derek G. Goring and Vladimir I. Nikora. J. Hydraul. Eng. 129 (6), 484–487.

Wall, L., Walters, L., Grizzle, R., Sacks, P., 2005. Recreational boating activity and its impact on the recruitment and survival of the oyster Crassostrea virginica on intertidal reefs in Mosquito Lagoon, Florida. J. Shellfish Res. https://doi.org/10.2983/0730-8000(2005)24[965:RBAAII]2.0.CO;2.

Walters, L.J., Phlips, E.J., Badylak, S., Mcclenahan, G., Sacks, P.E., Donnelly, M.J., 2021a. A negative association between recruitment of the eastern oyster Crassostrea virginica and the brown tide Aureoumbra lagunensis in Mosquito Lagoon, Florida. Florida Sci. 84 (2-3), 81–91.

Walters, L.J., Roman, A., Stiner, J., Weeks, D., 2001. Water Resource Management Plan, Canaveral National Seashore. Natl. Park Serv. Canaveral Natl. Seashore, Titusville, FL.

Walters, L.J., Sacks, P.E., Campbell, D.E., 2021b. Boating impacts and boat-wake resilient restoration of the eastern oyster Crassostrea virginica in Mosquito Lagoon, Florida, USA. Florida Sci. 84 (2-3), 173–199.

Whitman, E., Reidenbach, M., 2012. Benthic flow environments affect recruitment of Crassostrea virginica larvae to an intertidal oyster reef. Mar. Ecol. Prog. Ser. 463, 177–191. https://doi.org/10.3354/meps09882.

Wiberg, P.L., Taube, S.R., Ferguson, A.E., Kremer, M.R., Reidenbach, M.A., 2019. Wave attenuation by oyster reefs in shallow coastal bays. Estuar. Coasts 42 (2), 331–347.

Wildish, D., Kristmanson, D., 1997. Benthic Suspension Feeders and Flow. Cambridge University Press https://doi.org/10.1017/CBO9780511529894.

Wiles, P.J., Rippeth, T.P., Simpson, J.H., Hendricks, P.J., 2006. A novel technique for measuring the rate of turbulent dissipation in the marine environment. Geophys. Res. Lett. 33. https://doi.org/10.1029/2006GL027050.